Supporting materials

Deposited sulfur and reactive solid-phase iron measurements

Gravel samples were collected from three different layers (0.20, 0.32, and 0.44 m) before and after the batch experiment. Totally 100 g composited gravel was milled into a homogeneous powder with an agate ball mill (F-VD300, FOCUCY, Changsha, Hunan, China) and filtered using a mesh filter (100 mesh) for the analyses of deposited sulfur and reactive solid-phase iron. The composition of the deposited sulfur was measured using a sequential extraction method, according to Burton et al. (2006). The samples were initially treated with 1 mol/L hydrochloric acid in a distillation apparatus under permanent nitrogen gas flow. Acid volatile sulfide (AVS) was liberated as hydrogen sulfide, precipitated as zinc sulfide, and quantified using iodometric titration. Elemental sulfur was extracted by shaking the samples after AVS extraction with acetone for 24 h, followed by centrifugation (4000 g, 10 min), and the supernatant was transferred to a reagent bottle for pyrite-sulfur analysis by the Cr-reduction method (Sullivan et al., 2000). The acetone extract was vaporized to near-dryness at room temperature, and the elemental sulfur in the residue was determined with the Cr-reduction method. Reactive solid-phase iron(II) and iron(III) were recovered by anoxic extraction (20 h in the dark) with 0.2 mol/L NH4-oxalate/oxalic acid (adjusted to pH 3) (Phillips and Lovley, 1987) and analyzed by the 1,10-phenanthroline method (APHA, 1998).

Plant uptake estimation

A total of 10 g of aboveground and belowground plant material was collected from four sampling areas (10 cm × 10 cm) in the microcosms before and after the batch experiment. After collection, the samples were cleaned, dried, milled into homogeneous powders, and filtered using a mesh filter (200 mesh). Sulfur content was analyzed with an elemental analyzer (Vario EL III, Elementar, Hanau, Germany). Total biomass was estimated by measuring the number and height of the stems. The relationship between the biomass dry weight and the stem height was obtained by measuring the heights and dry weights of all the stems in the constructed wetlands (CWs) after the batch experiment. Plant uptake rate was calculated from the total aboveground and belowground biomass and their sulfur contents.

^{15}N-isotope measurement

For the ^{15}N-isotope measurements, samples were prepared according to Silva et al. (2000). Anion-exchange resins (AG 1-X8, 100–200 mesh size; Bio-Rad, Hercules, CA, USA) were used to collect, transport, and enrich the water samples for the analysis of nitrogen isotope in nitrate. The $AgNO_3$ extracted from the anion exchange resin was freeze-dried and combusted in an elemental analyzer and continuously transferred into an isotope ratio mass spectrometer (Thermo Fisher Mat 253, Thermo Fisher Scientific, Waltham, MA, USA). ^{15}N-isotope measurements were performed with an analytical error of ± 0.5‰ or better.

Analysis of bacterial community by 454 high-throughput 16S rRNA gene pyrosequencing

Bacterial 16S rRNA genes for pyrosequencing were amplified by PCR using a 10-nucleotide barcoded forward primer 8F (5′-AGAGTTTGATCCTGGCTCAG-3′) and reverse primer 533R (5′-TTACCGCGGCTGCTGGCAC-3′), which targeted the V1–V3 region. The 20 μL PCR mixture contained 4 μL of 5 × FastPfu Buffer, 2 μL of 2.5 mmol/L dNTPs, 0.4 μL of each primer (5 μmol/L), 0.5 μL of DNA, and 0.4 μL FastPfu Polymerase (TransStart FastPfu DNA Polymerase, TransGen, China). The thermocycling steps were as follows: 95℃ for 2 min, followed by 25℃ cycles at 95℃ for 30 s, 55℃ for 30 s, 72℃ for 30 s and a final extension step at 72℃ for 5 min. After purification using the UNIQ-10 PCR Purification Kit (Sangon, Shanghai, China) and quantification using a TBS-380 (Turner BioSystems, Inc., USA), a mixture of amplicons was used for pyrosequencing on a Roche massively parallel 454 GS-FLX Titanium sequencer (Roche 454 Life Sciences, Bran-ford, CT, USA) according to standard protocols. To minimize the effects of random sequencing errors, low-quality sequences were removed by eliminating those without an exact match to the forward primer, without a recognizable reverse primer, of length shorter than 150 nucleotides and containing any ambiguous base calls (Ns). The barcodes and primers were trimmed from the resulting sequences. Finally, a total of 39445 high-quality sequence tags were produced, with an average length of 469 bp per sequence. The operational taxonomic units (OTUs) were clustered with 97% similarity using the MOTHUR program. Rarefaction curves, species richness estimator (Chao1), Shannon diversity index, and Good's coverage were generated in MOTHUR for each sample. BLAST of taxonomic classification down to the phylum, class and genus level was then achieved using MOTHUR via the SILVA 106 database with a set confidence threshold of 80%. Abundance of a given phylogenetic group was set as the number of sequences affiliated with that group divided by the total number of sequences per sample.

Table S1 Detection limits, relative standard deviations, and recoveries for the analytical methods used in this study

Parameter		Detection limit	Relative standard deviation ($n \geq 3$)	Recovery
Aqueous parameter	Sulfide	0.1 mg S/L[a], 0.02 mg S/L[b]	< 20.0%[a], < 5.4%[b,c]	89%–92%[a], 80%–97%[b], 92%–95%[c]
	Iron	0.01 mg Fe/L[a], 0.03 mg Fe/L[b]	< 25.5%[a], < 1.0%[b], < 7.8%[c]	97.4%–102.6%[b], 88.0%–98.0%[c]
	Sulfate	0.03 mg S/L[a,b], 0.02 mg S/L[d]	< 6.1%[a], < 8.1%[b], < 7.4%[c], < 4.6[d]	86.7%–113.0%[a], 92.1%–104.9%[c], 91.5%–114.5%[d]
	Sulfite	0.03 mg S/L[c], 0.02 mg S/L[d]	< 5.8%[d]	82.3%–106.0%[d]
	Thiosulfate	0.003 mg S/L[e]	< 8.1%[c], < 1.5%[e]	93.1%–114%[c], 96.4%–100%[e]
	Nitrate	0.02 mg N/L[a,b], 0.004 mg N/L[d]	< 7.5%[a], < 4.6%[b], < 6.1%[c], < 5.1%[d]	95.0%–111.5%[b], 91.3%–104.3%[c], 91.7%–108.3%[d]
	Nitrite	0.03 mg N/L[a], 0.01 mg N/L[b], 0.005 mg N/L[d]	< 3.9%[a], < 9.6%[b], < 9.7%[c], < 4.4%[d]	89.6%–113.1%[b], 92.8%–110.1%[c], 89.5%–113.2%[d]
	Ammonia	0.02 mg N/L[f,g]	< 9.4%[c], < 3.4%[f], < 6.0%[g]	93.5%–102.6%[c], 90%–104%[f], 93%–111%[g]
	Polysulfide	0.03–0.30 mg S/L[h,i]	< 32%[h,i]	94.0%–100%[h,i]
	Elemental sulfur	0.06 mg S/L[j]	< 18.7%[j]	–
	Total nitrogen	0.05 mg N/L[b]	< 2.5%[b], < 3.8%[c]	95%–105%[b], 91.3%–103.0%[c]
	COD	5 mg COD/L[a], 4 mg COD/L[k]	< 5.6%[a], < 4.7%[c], < 11%[k]	90%–111%[c], 94.2%–103.5%[k]
	Total sulfur	0.1 mg S/L[l]	< 9.7%[c], < 5.0%[l]	94.2%–97.5%[c], 95.5%–104.9%[l]
	Calcium ion	0.01 mg /L[a], 0.002 mg /L[b]	< 5.0%[a], < 2.2%[b], < 3.1%[c]	95%–105%[a], 94.5%[b], 95.2%–98.3%[c]
Gaseous parameter	Hydrogen sulfide	0.105 ug[m]	< 4.3%[m]	–
Solid parameter	AVS	0.001 mg S[c]	< 5.5%[c]	88.6%–93.4%[c]
	Pyrite	0.001 mg S[c]	< 4.6%[c]	91.5%–103.4%[c]
	Elemental sulfur	0.001 mg S[c]	< 6.4%[c]	87.3%–98.4%[c]
	Iron(II)	0.00025 mg Fe[c]	< 6.9%[c]	92.2%–109.3%[c]
	Iron(III)	0.00025 mg Fe[c]	< 6.7%[c]	89.5%–95.1%[c]
	Sulfur content in plants	0.0005 mg S[c]	< 1.2%[c]	96.1%–98.3%[c]

Notes: a) Data from APHA (1998), b) SEPA (2004), c) this study, d) MEP (2016), e) Miura et al. (1998), f) Ferreira et al. (2017), g) Ferreira et al. (2016), h) Kamyshny et al. (2006), i) Kamyshny et al. (2009), j) Rethmeier et al. (1997), k) MEP (2017), l) Sarudi and Kelemen (1998), and m) Venturi et al. (2016); –, not available

Table S2 Calculation methods for the average rates of net sulfur deposition, plant uptake, and hydrogen sulfide volatilization

Processes	Rates calculation	Equation No.
Sulfur deposition	$R_{deposition} = R_{AVS,deposition} + R_{pyrite,deposition} + R_{ES,deposition}$	(S1)
	$R_{AVS,deposition} = (M_{AVS,final} - M_{AVS,initial}) \cdot V_b^{-1} \cdot nT^{-1}$	(S2)
	$R_{pyrite,deposition} = (M_{PS,final} - M_{PS,initial}) \cdot V_b^{-1} \cdot nT^{-1}$	(S3)
	$R_{ES,deposition} = (M_{ES,final} - M_{ES,initial}) \cdot V_b^{-1} \cdot nT^{-1}$	(S4)
Plant uptake	$R_{plant\ uptake} = (C_{S,final} \cdot M_{plant,final} - C_{S,initial} \cdot M_{plant,initial}) \cdot V_b^{-1} \cdot nT^{-1}$	(S5)
Hydrogen sulfide volatilization	$R_{volatilization} = m \cdot Q_k^{-1} \cdot T_e^{-1} \cdot T^{-1}$	(S6)

Notes: $R_{AVS,deposition}$, $R_{pyrite,deposition}$, and $R_{ES,deposition}$ are the average net deposition rates of AVS, pyrite, and elemental sulfur (g S/(m^3·d)), respectively; V_b is the bed volume of the microcosm (m^3); n is the total number of batches; T is the retention time of each batch (days); $M_{AVS,initial}$, $M_{pyrite,initial}$, and $M_{ES,initial}$ are the mass of AVS, pyrite, and elemental sulfur before the batch experiment (g S), respectively; $M_{AVS,final}$, $M_{pyrite,final}$, and $M_{ES,final}$ are the mass of AVS, pyrite, and elemental sulfur after the batch experiment (g S), respectively; $R_{plant\ uptake}$ is the average plant sulfur uptake rate (g S/(m^3·d)); $C_{S,initial}$ and $C_{S,final}$ are the sulfur contents in the plants before and after the batch experiment (g S/g), respectively; $M_{plant,initial}$ and $M_{plant,final}$ are the mass of plants before and after the batch experiment (g), respectively; $R_{volatilization}$ is the average volatilization rate of hydrogen sulfide (g S/(m^3·d)); m is the mass of hydrogen sulfide trapped in the adsorbing cartridge of passive sampler (μg S); Q_k is the sampling rate of hydrogen sulfide at 298 K (mL/min, Q_k = 69 mL/min); and T_e is the exposure time of passive sampler to hydrogen sulfide (min, T_e = 7200 min)

Table S3 Calculation methods for electron transfer rates and efficiency of sulfur cycle-mediated electron transfer

Processes	Rates calculation	Equation No.
Electron input	$r_{input} = R_{COD,input} \cdot n_{COD}$	(S7)
Electron acceptance	$r_{oxygen,acceptance} = R_{oxygen\ uptake} \cdot n_{oxygen}$	(S8)
	$r_{nitrate,acceptance} = R_{denitrification} \cdot n_{nitrate}$	(S9)
	$r_{iron,acceptance} = R_{iron\ reduction} \cdot n_{iron}$	(S10)
	$r_{sulfate,acceptance} = R_{sulfate\ reduction} \cdot n_{sulfate}$	(S11)
Electron storage	$r_{AVS,storage} = (R_{AVS,deposition} + R_{AVS,oxidation}) \cdot n_{AVS}$	(S12)
	$r_{pyrite,storage} = R_{pyrite,deposition} \cdot n_{pyrite}$	(S13)
	$r_{ES,storage} = (R_{ES,deposition} + R_{ES,oxidation}) \cdot n_{ES}$	(S14)
Electron donation	$r_{AVS,donation} = R_{AVS,oxidation} \cdot n_{AVS}$	(S15)
	$r_{ES,donation} = R_{ES,oxidation} \cdot n_{ES}$	(S16)
Electron transfer efficiency	$\eta_e = (r_{AVS,donation} + r_{ES,donation}) / r_{sulfate,acceptance} \cdot 100\%$	(S17)

Notes: r_{input} is the electron input rate by organics in the influent (mol/(m^3·d)); $r_{oxygen,acceptance}$, $r_{nirate,acceptance}$, $r_{iron,acceptance}$, and $r_{sulfate,acceptance}$ are the electron acceptance rates of dissolved oxygen, nitrate, iron(III), and sulfate (mol/(m^3·d)), respectively; $R_{oxygen\ uptake}$ is oxygen uptake rate (g O_2/(m^3·d)); $R_{denitrification}$ is denitrification rate (g N/(m^3·d)); $R_{iron\ reduction}$ is iron reduction rate (g Fe/(m^3·d)); $R_{sulfate\ reduction}$ is sulfate reduction rate (g S/(m^3·d)); $r_{AVS,storage}$, $r_{pyrite,storage}$, and $r_{ES,storage}$ are the electron storage rates of AVS, pyrite, and elemental sulfur (mol/(m^3·d)), respectively; $r_{AVS,donation}$ and $r_{ES,donation}$ are the electron doantion rates of AVS and elemental sulfur (mol/(m^3·d)), respectively; n_{COD}, n_{oxygen}, $n_{nitrate}$, n_{iron}, $n_{sulfate}$, n_{AVS}, n_{pyrite}, and n_{ES} are electron equivalents of per gram of COD, oxygen, nitrate, iron, sulfate, AVS, pyrite-sulfur, and elemental sulfur (mol/g, n_{COD} = 0.125 mol/g COD, n_{oxygen} = 0.125 mol/g O_2, $n_{nitrate}$ = 0.357 mol/g N, n_{iron} = 0.018 mol/g Fe, $n_{sulfate}$ = 0.250 mol/g S, n_{AVS} = 0.250 mol/g S, n_{pyrite} = 0.219 mol/g S, and n_{ES} = 0.188 mol/g S); and η_e is the electron transfer efficiency of sulfur cycle

Table S4 Calculation methods for the rates of oxygen uptake, sulfate reduction, and iron reduction

Processes	Rates calculation	Equation No.	References
Reaeration	$R_{\text{reaeration}} = \mathrm{k_{La}} \cdot \int_{t}^{t+\Delta t} \left(\mathrm{S_{osat}} - S_{\mathrm{o,t}}\right) \mathrm{d}t \cdot V_{\mathrm{w}} \cdot V_{\mathrm{b}}^{-1} \cdot \Delta t^{-1}$	(S18)	(Rousseau, 1978)
Plant leaching	$R_{\text{plant leaching}} = \left(\mathrm{K_{ROL\text{-}L}} \cdot \Delta t_{\mathrm{L}} + \mathrm{K_{ROL\text{-}D}} \cdot \Delta t_{\mathrm{D}}\right) \cdot M_{\text{root}} \cdot M_{\mathrm{r}} \cdot V_{\mathrm{b}}^{-1} \cdot \Delta t^{-1} \cdot 8.6 \cdot 10^{-4}$	(S19)	(Matsui and Tsuchiya, 2006)
Oxygen uptake	$R_{\text{oxygen uptake}} = R_{\text{reaeration}} + R_{\text{plant leaching}} - \left(S_{\mathrm{o,t+\Delta t}} - S_{\mathrm{o,t}}\right) \cdot V_{\mathrm{w}} \cdot V_{\mathrm{b}}^{-1} \cdot \Delta t^{-1} \cdot 24$	(S20)	
Sulfate reduction	$R_{\text{sulfate reduction}} = R_{\text{sulfate removal}} - R_{\text{plant uptake}}$	(S21)	
	$R_{\text{sulfate reduction,t}} = -\frac{\mathrm{d}C_{\text{sulfate,t}}}{\mathrm{d}t} \cdot V_{\mathrm{w}} \cdot V_{\mathrm{b}}^{-1} \cdot 24 - R_{\text{plant uptake}}$	(S22)	
Iron reduction	$R_{\text{iron reduction}} = \left(M_{\text{iron(III),final}} - M_{\text{iron(III),initial}}\right) \cdot V_{\mathrm{b}}^{-1} \cdot n \cdot T^{-1}$	(S23)	

Notes: $R_{\text{reaeration}}$, $R_{\text{plant leaching}}$, and $R_{\text{oxygen uptake}}$ are the average physical reaeration, plant leaching, and oxygen uptake rates between t and $t + \Delta t$ (g O_2/(m^3·d)), respectively; k_{La} is the oxygen mass transfer coefficient (d^{-1}, k_{La} = 0.1 d^{-1}); V_w is the working volume of the microcosm (m^3); V_b is the bed volume of the microcosm (m^3); Δt is the duration of the target phase (hours); S_{osat} is the saturated dissolved oxygen concentration (mg/L, S_{osat} = 8.25 mg/L); $S_{o,t}$ and $S_{o,t+\Delta t}$ are the dissolved oxygen concentrations at time t and $t + \Delta t$ (mg/L), respectively; $K_{ROL\text{-}L}$ and $K_{ROL\text{-}D}$ are the constants of root oxygen loss in the light and dark (nmol O_2/(g DW_{root}·s), $K_{ROL\text{-}L}$ = 0.33 nmol O_2/(g DW_{root}·s), $K_{ROL\text{-}D}$ = 0.18 nmol O_2/(g DW_{root}·s)), respectively; Δt_L and Δt_D are the durations of light and dark periods (hours), respectively; M_{root} is the total roots dry weigh of plants (g); M_r is the relative molecular mass of oxygen (g/mol); $R_{sulfate\ removal}$ is the average sulfate removal rate (g S/(m^3·d)); $R_{sulfate\ reduction,t}$ is the sulfate reduction rate at time t (g S/(m^3·d)); $C_{sulfate,t}$ is the sulfate concentration at time t (mg S/L); and $M_{iron(III),initial}$ and $M_{iron(III),final}$ are the mass of reactive iron(III) in the microcosm before and after the batch experiment (g Fe)

Table S5 Estimated species richness and diversity of samples

Parameter	Value
Coverage (%)	94
Ace	4867.89
Chao 1	4572.22
Shannon	6.22
Simpson	0.0097

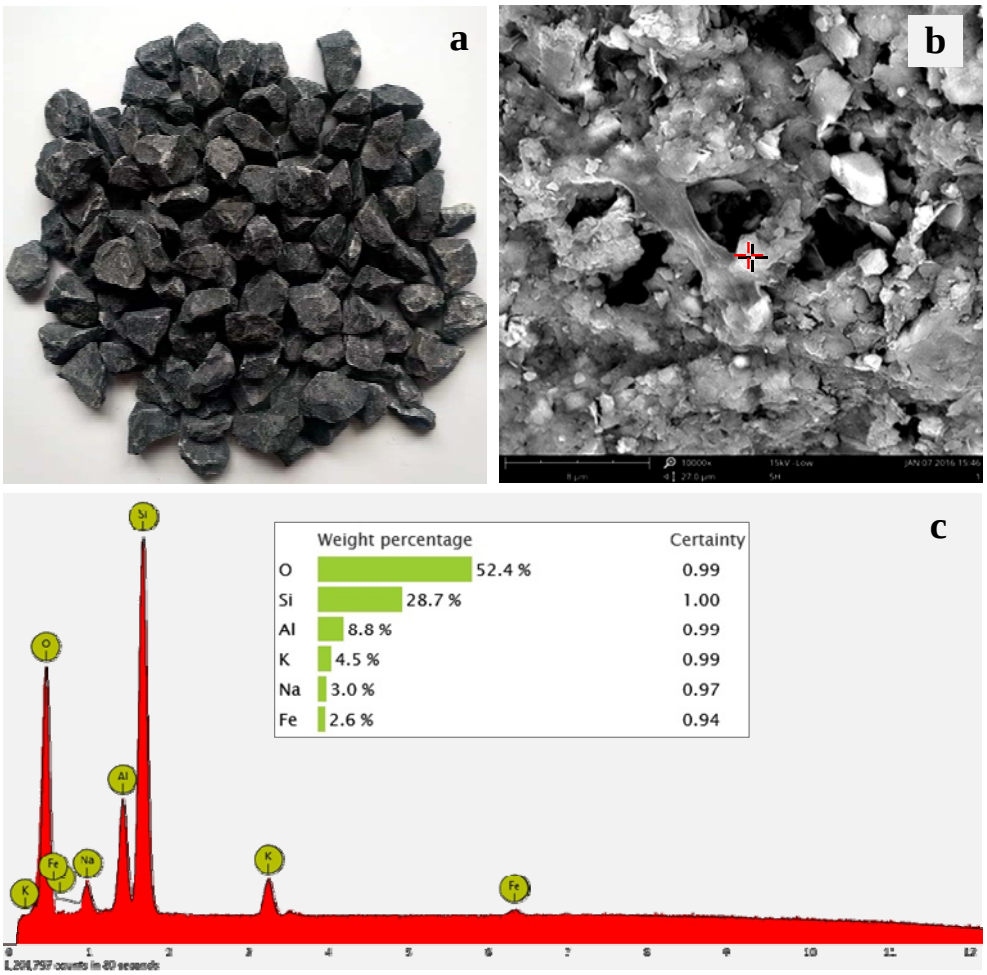

Fig. S1 Appearance (a), SEM image (b), and EDS spectra (c) of fresh gravel

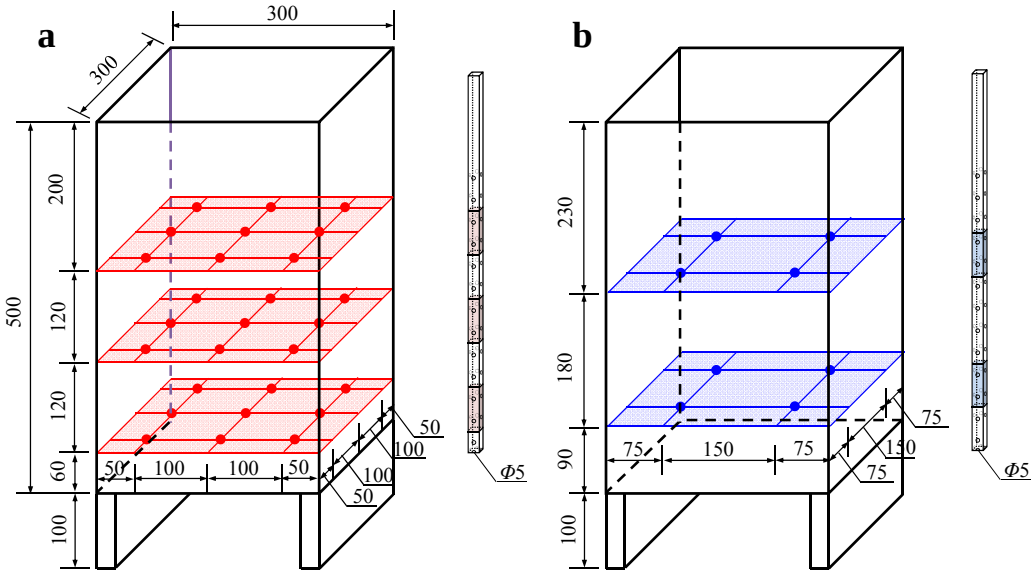

Fig. S2 Schematic diagram of the CW microcosm, sampling points, and the sampling tools for collecting samples for analyses of the deposited sulfur and reactive solid-phase iron (a) and microbial community (b). At each sampling point, 13.5 cm^3 (1.5 × 1.5 × 6 cm) of gravel were collected

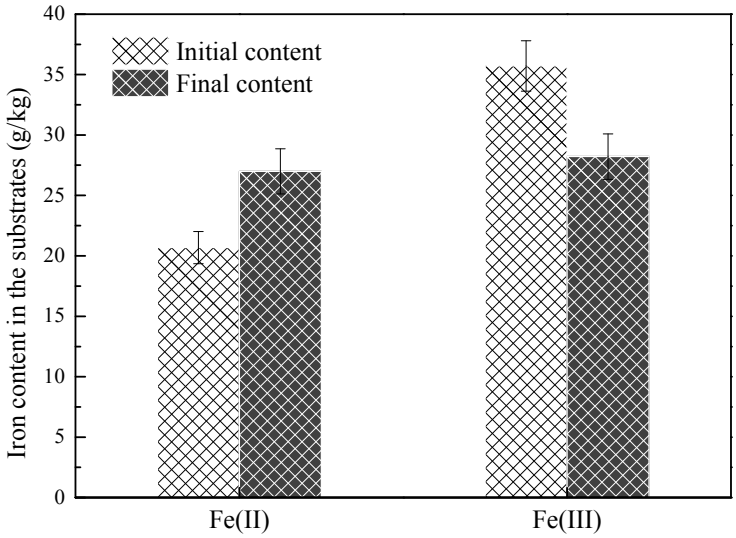

Fig. S3 Reactive solid-phase iron(II) and iron(III) contents in the substratum before (initial content) and after (final content) the batch experiments. Error bars represent ± standard deviation (n = 3)

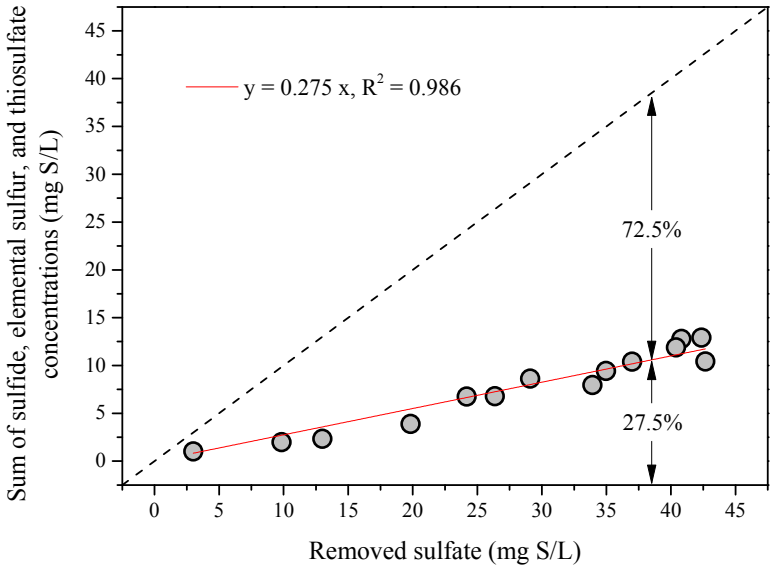

Fig. S4 Correlations between the removed sulfate and the sum of sulfide, elemental sulfur, and thiosulfate in the pore water. The straight dotted line illustrates the theoretical correlation for a complete accumulation of reduced sulfur reservoir. The straight solid line illustrates the regression of measured reduced sulfur in the pore water

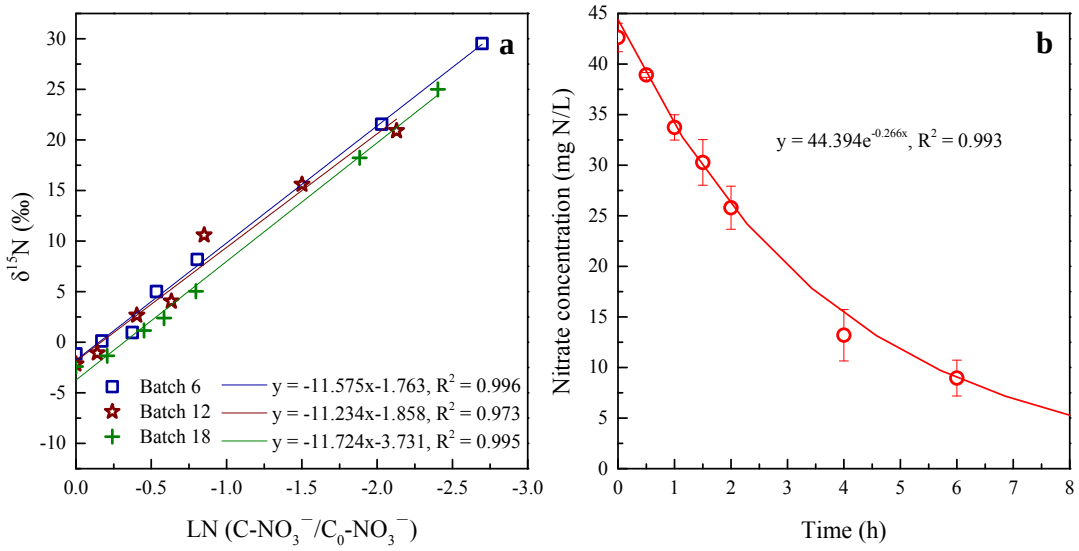

Fig. S5 Correlation of the $\delta^{15}N$ value in nitrate and the residual nitrate fraction (a) and the variation of nitrate concentration under pure denitrification (b)

References

APHA (1998). Standard Methods for the Examination of Water and Wastewater, 20th ed. Washington, DC: American Public Health Association

Burton E D, Bush R T, Sullivan L A (2006). Reduced inorganic sulfur speciation in drain sediments from acid sulfate soil landscapes. Environmental Science & Technology, 40(3): 888–893

Ferreira F N, Afonso J C, Pontes F V, Carneiro M C, Neto A A, Tristao M L, Monteiro M I (2016). Determination of low-molecular-weight amines and ammonium in saline waters by ion chromatography after their extraction by steam distillation. Journal of Separation Science, 39(8): 1454–1460

Ferreira F N, Afonso J C, Pontes F V M, Carneiro M C, Neto A A, Junior R E, Monteiro M I C (2017). Ultrasound-assisted purge-and-trap extraction for simultaneous determination of low-molecular weight amines and ammonium in high salinity waters by ion chromatography. Microchemical Journal, 133: 658–662

Kamyshny A, Borkenstein C G, Ferdelman T G (2009). Protocol for quantitative detection of elemental sulfur and polysulfide zero-valent sulfur distribution in natural aquatic samples. Geostandards and Geoanalytical Research, 33(3): 415–435

Kamyshny A, Ekeltchik I, Gun J, Lev O (2006). Method for the determination of inorganic polysulfide distribution in aquatic systems. Analytical Chemistry, 78(8): 2631–2639

Matsui T, Tsuchiya T (2006). A method to estimate practical radial oxygen loss of wetland plant roots. Plant Soil, 279(1–2): 119–128

MEP (2016). HJ 84-2016 Water Quality-Determination of Inorganic Anions (F^-, Cl^-, NO_2^-, Br^-, NO_3^-, PO_4^{3-}, SO_3^{2-}, SO_4^{2-})-Ion Chromatography. Beijing: Chinese Environment Science Press (in Chinese)

MEP (2017). HJ 828-2017 Water Quality-Determination of Chemical Oxygen Demand-Dichromate Method. Beijing: Chinese Environment Science Press (in Chinese)

Miura Y, Fukasawa K, Koh T (1998). Determination of sulfur anions at the ppb level by ion chromatography utilizing their catalytic effects on the postcolumn reaction of iodine with azide. Journal of Chromatography A, 804: 143–150

Phillips E J P, Lovley D R (1987). Determination of Fe(III) and Fe(II) in oxalate extracts of sediment. Soil Science Society of America Journal, 51(4): 938–941

Rethmeier J, Rabenstein A, Langer M, Fischer U (1997). Detection of traces of oxidized and reduced sulfur compounds in small samples by combination of different high-performance liquid chromatography methods. Journal of Chromatography A, 760(2): 295–302

Rousseau D (1978). Performance of constructed treatment wetlands: model-based evaluation and impact of operation and maintenance. Biological Psychology, 51(1): 59–76

Sarudi I, Kelemen J (1998). Determination of sulfur and total sulfur dioxide in wines by an ICP-AES method. Talanta, 45(6): 1281–1284

SEPA (2004). Monitoring and Analysis Method of Water and Waste Water, 4th ed. Beijing: Chinese Environment Science Press (in Chinese)

Silva S R, Kendall C, Wilkison D H, Ziegler A C, Chang C C Y, Avanzino R J (2000). A new method for collection of nitrate from fresh water and the analysis of nitrogen and oxygen isotope ratios. Journal of Hydrology, 228(1): 22–36

Sullivan L A, Bush R T, Mcconchie D M (2000). A modified chromium-reducible sulfur method for reduced inorganic sulfur: Optimum reaction time for acid sulfate soil. Australian Journal of Soil Research, 38(3): 729–734

Venturi S, Cabassi J, Tassi F, Capecchiacci F, Vaselli O, Bellomo S, Calabrese S, D'alessandro W (2016). Hydrogen sulfide measurements in air by passive/diffusive samplers and high-frequency analyzer: A critical comparison. Applied Geochemistry, 72: 51–58